

Dynamic AFM Elastography Reveals Phase Dependent Mechanical Heterogeneity of Beating Cardiac Myocytes

Evren U. Azeloglu and Kevin D. Costa

Abstract—We developed a novel atomic force microscope (AFM) indentation technique for mapping spatiotemporal stiffness of spontaneously beating neonatal rat cardiac myocytes. Cells were indented at a rate close but unequal to their contractile frequency. Resultant apparent elastic modulus cycled at a predictable envelope frequency between a systolic value of 26.2 ± 5.1 kPa and a diastolic value of 7.8 ± 4.1 kPa. In cells probed along their axis, spatial heterogeneity of systolic stiffness correlated with the sarcomeric structure of underlying myofibrils. Treatment with blebbistatin eliminated contractile activity and resulted in a uniform modulus of 6.5 ± 4.8 kPa. The technique provides a unique means of probing the mechanical effects of disease processes and pharmacological treatments on beating cardiomyocytes at the subcellular level, providing new insights relating myocardial structure and function.

I. INTRODUCTION

THE cellular constituents of the myocardium undergo significant structural changes throughout each cardiac cycle. The resultant periodic alterations of heart muscle mechanics directly affect cardiac function and play an important role in our understanding of cardiac physiology.

Prior studies of cardiomyocyte biomechanics have focused on axial properties, though transverse properties also impact pump function [2] and active force generation [5]. The few studies on transverse mechanics of intact heart muscle [6], individual cardiomyocytes [7] or isolated cardiac myofibrils [1] have used chemically stabilized conditions, mainly due to technical challenges with actively beating samples. Because local micromechanics can influence cardiac cell function [8, 9], it is important to understand how mechanical properties vary spatially with subcellular location, as well as temporally throughout cyclic activation and relaxation. Such data are also required for multi-scale computational models of the heart [10].

The atomic force microscope (AFM) has been utilized to investigate micromechanics of various cell types, including passive cardiac myocytes [3, 11, 12]. Only two AFM studies probed dynamic properties of neonatal cardiomyocytes; one demonstrated subcellular regional heterogeneity of pulse rate [13], and the other showed AFM tip resonance behavior qualitatively reflecting periodicity of cell stiffness [14]. Recent AFM studies of isolated cardiac myofibrils revealed

local heterogeneities in transverse stiffness during rigor, with z-bands significantly stiffer than other sarcomeric structures [1]. However, it is unknown whether myofibrillar mechanical heterogeneity translates to an intact myocyte and thereby to adjacent cells. If so, subcellular micromechanical heterogeneity could potentially impact key aspects of cardiac structure and function such as transverse force generation, electromechanical coupling, and registration of sarcomeres across neighboring cardiomyocytes.

No prior studies have quantified subcellular mechanics of living cardiomyocytes in physiologically relevant, dynamic conditions. Therefore, the goal of this study is to introduce a novel AFM-based method to characterize spatiotemporal heterogeneity of subcellular micromechanical properties in spontaneously beating cardiac myocytes, opening new avenues of research into the biochemical and biophysical properties of the contractile machinery in the heart.

II. MATERIALS AND METHODS

A. Cell Isolation and Culture

All animal protocols were approved by the Institutional Animal Care and Use Committee at Columbia University. Chemicals were purchased from Sigma-Aldrich (St. Louis, MO) unless otherwise noted. Neonatal rat cardiac myocytes (NRCM) were isolated by serial enzymatic digestion of minced ventricles from day-2 Sprague-Dawley rats (Taconic Farms, Germantown, NY) as previously described [15], and were plated on culture dishes brushed with bovine type-I collagen (Inamed Biomaterials, Fremont, CA). Attached cells formed aligned myofibrils with registered sarcomeres, and started spontaneous contractions at 3-4 Hz within 24-48 hours of plating. NRCM were cultured under standard conditions with DMEM and 10% neonatal bovine serum (Hyclone, Logan, UT) for 5-20 days prior to AFM studies.

B. Experimental Protocol

A Bioscope AFM (Veeco, Santa Barbara, CA) coupled with an inverted confocal microscope (Olympus, Center Valley, PA) and heated stage was used to probe spontaneously beating NRCM at 37°C. A pyramid-tipped silicon nitride AFM probe was mounted on a fluid cell with a silicone skirt to prevent evaporation. Visibly contracting NRCM ($n = 8$ from separate dishes) were repeatedly indented over a central region at a frequency nearly equal to the cell pulse rate. Synchronized high-speed video microscopy (Redlake, San Diego, CA) yielded the time of AFM indentation relative to the phase of contraction. The

Manuscript received April 22, 2009. This work was supported in part by the National Science Foundation CAREER Award BES-0239138.

EUA (evren.azeloglu@mssm.edu) and KDC (kevin.costa@mssm.edu) were formerly with the Department of Biomedical Engineering at Columbia University. They are now with the Cardiovascular Research Center in the Department of Medicine (Cardiology) at Mount Sinai School of Medicine, New York, NY 10029 USA (phone: 212-241-7122; fax: 212-241-4080).

frequency of cellular contraction was quantified from these images by fast-Fourier transform of the time course of axial cell displacement, determined using a published phase correlation algorithm [16]. The convolution of the AFM indentation frequency (f_{AFM}) and the myocyte pulse rate (f_{cell}) created a response signal with a third envelope frequency ($f_{envelope}$) equal to the difference of the two input frequencies,

$$f_{envelope} = f_{cell} - f_{AFM} \quad (1)$$

Indentations were repeated over multiple subcellular locations, providing a spatiotemporal mechanical map of the myocyte. Some NRCM ($n = 4$) were treated with 100 μ M blebbistatin for 20 min to arrest contraction, and then probed again. Other cells ($n = 4$) were probed over a 12- μ m linear array with 1/3 μ m step size, aligned with the major cell axis, to correlate myocyte mechanics with underlying sarcomeric structures. Finally, cells were fixed in 3.7% formaldehyde, rinsed with PBS, permeabilized with 0.05% triton-X and stained with anti- β -tubulin antibody, rhodamine-conjugated phalloidin (Invitrogen, Carlsbad, CA) and DAPI dilactate.

C. Data Analysis

AFM force curves were analyzed as previously described [17]. Briefly, each raw deflection-extension curve was parsed into pre- and post-contact regions by fitting a bi-domain linear-quadratic function to identify the contact point. The origin was reset to this contact point to obtain the force-indentation curve, and the depth-dependent apparent elastic modulus was computed using

$$\hat{E}_{app}(D) = F(D) / (2\pi \phi(D)) \quad (2)$$

where $\phi(D)$ is a depth-dependent geometric function for a blunt-cone indenter; $F(D)$ is the instantaneous indentation force obtained by multiplying probe deflection with the cantilever spring constant; and $\hat{E}_{app}(D)$ is the depth-dependent pointwise apparent elastic modulus, which can be related to the Young's modulus, E , of an equivalent linear elastic substrate via $\hat{E}_{app} = E / 2(1 - \nu^2)$, where a Poisson's ratio of $\nu = 0.5$ is often used assuming material incompressibility of the cell. During post-processing, the timing of each indentation in relation to the contractile phase of the myocyte was determined. Data were pooled together from multiple contraction cycles to obtain a mean stiffness value during systolic shortening and diastolic relaxation for each cell. Data are presented as mean \pm standard deviation for $n = 8$ cells unless otherwise specified. Modulus values were compared using one-way analysis of variance (ANOVA) and Tukey's post-hoc test with statistical significance accepted for $p < 0.05$.

III. RESULTS AND DISCUSSION

A. Spatiotemporal Mapping of Cardiomyocyte Mechanics

All tested myocytes contracted spontaneously (i.e. without electrical pacing), with a mean f_{cell} of 3.6 ± 1.0 Hz. When probed repeatedly at an indentation frequency close but

unequal to the pulse rate ($f_{AFM} = 3.9 \pm 1.4$ Hz; $f_{envelope} = 1.0 \pm 0.6$ Hz), the relative timing of each AFM indentation shifted along the cardiomyocyte twitch cycle. This resulted in a sequence of indentations mapping out the temporal changes in mechanical state at a given spatial location within the cell. For example (see **Fig. 1A**), when f_{AFM} (4.35 Hz) exceeded f_{cell} (4.10 Hz), and the first indentation coincided with the end of a contraction, the second indentation occurred at a slightly earlier time point during the twitch cycle, and so on for subsequent indentations. Accordingly, the resultant \hat{E}_{app} values at the given indentation site cyclically changed with $f_{envelope}$ of 0.25 Hz (**Eq. 1**). NRCM stiffness values, obtained over 3-4 envelope cycles, or 10-15 contractions for each cell, had a mean systolic pointwise modulus of 26.2 ± 5.1 kPa at a representative indentation depth of 400 nm, which was significantly different from the corresponding diastolic modulus of 7.8 ± 4.1 kPa ($p < 0.01$, **Fig. 1C, D**).

In myocytes indented along the major axis of contraction (**Fig. 1E**), spatiotemporal modulus maps revealed greater variability during systole than diastole, with the standard deviation of intracellular modulus values being 6.9 ± 4.4 kPa during systole versus 2.0 ± 1.2 kPa during diastole ($p < 0.01$; **Fig. 1F**). Thus, whereas the passive myocyte is mechanically relatively soft and uniform, contraction not only increases stiffness but also induces periodic nonuniformity of elastic properties along the length of the cell. There was a significant correlation between the spatial elasticity pattern during systole and the underlying sarcomeric actin staining ($r^2=0.52$, $p<0.01$), with approximately 2 μ m spacing between periodic stiff sites (**Fig. 1F**). These data represent the first *in vitro* observations of transverse stiffness heterogeneity in living beating cardiomyocytes, which had previously only been reported in isolated myofibrils [1].

B. Blebbistatin Effects

Treatment of cells with blebbistatin abruptly stopped contractions within a few minutes, and reduced the average pointwise modulus to diastolic values; mean \hat{E}_{app} at 400 nm depth was 6.5 ± 4.8 kPa ($n = 4$), which was significantly different than pre-treatment systolic ($p < 0.01$) but not diastolic ($p = 0.89$) modulus. Unlike arresting agents such as 2-3-butanedione monoxime (BDM), which can have non-specific effects on cardiomyocyte viability and function, blebbistatin slows ATP hydrolysis within the myosin motor [18], inhibiting active force generation and preventing contraction without disrupting the underlying sarcomeric structure. Prevention of systolic stiffening by blebbistatin treatment strengthens the conclusion that changes in elastic modulus observed in isolated beating cardiomyocytes were due to activation of actin-myosin crossbridges.

C. Comparison with Previous Studies

Table 1 summarizes Young's modulus values reported for several rat cardiac structures measured using AFM. For comparison, a Poisson's ratio of 0.5 was used to convert our pointwise apparent modulus to an equivalent elastic Young's

modulus, E (see METHODS). Neonatal rat cardiac myofibrils were approximately 3- to 5-fold stiffer when isolated on glass [1] than when embedded within the cytoplasmic milieu of beating cardiomyocytes, although sarcomere-related mechanical heterogeneity could still be detected in the intact cell. The diastolic NRCM modulus was also 3 to 3.5 times softer than that for isolated passive adult cardiomyocytes [3], which may reflect more densely packed myofibrils in adult cells, as well as increased cardiomyocyte stiffness with aging. Finally, non-infarcted adult rat myocardium [4] exhibited a Young's modulus intermediate between the diastolic and systolic values obtained in the present study, possibly indicating partial contracture of the sectioned myocardial tissue sample during testing in culture media.

No prior AFM studies have quantified the systolic stiffness of cardiomyocytes or myocardium. However, the mean ratio of systolic to diastolic stiffness of beating myocytes in the present study was 4.4 ± 2.7 , compared to corresponding ratio values ranging from about 10 for

sectioned adult rabbit myocardium [5], to nearly 40 in the beating human heart [19]. The discrepancy could reflect factors such as extracellular matrix contributions, cell-cell interactions, or 3-D structural and mechanical anisotropy, none of which are present in isolated myocyte cultures. Also, because cardiomyocyte stiffness increases with age [3], development from neonate to adult may also alter mechanical properties of the heart. In principle, our AFM technique could also be applied to the beating neonatal heart for direct comparison of cardiomyocyte and myocardial diastolic and systolic properties. Such multi-scale studies could relate ventricular chamber stiffness to intrinsic cellular mechanical properties, which is essential for understanding mechanisms of heart failure and remodeling.

D. Limitations

The method developed herein combines AFM stiffness data from multiple cardiomyocyte contractions to form a single time-dependent mechanical profile at a particular

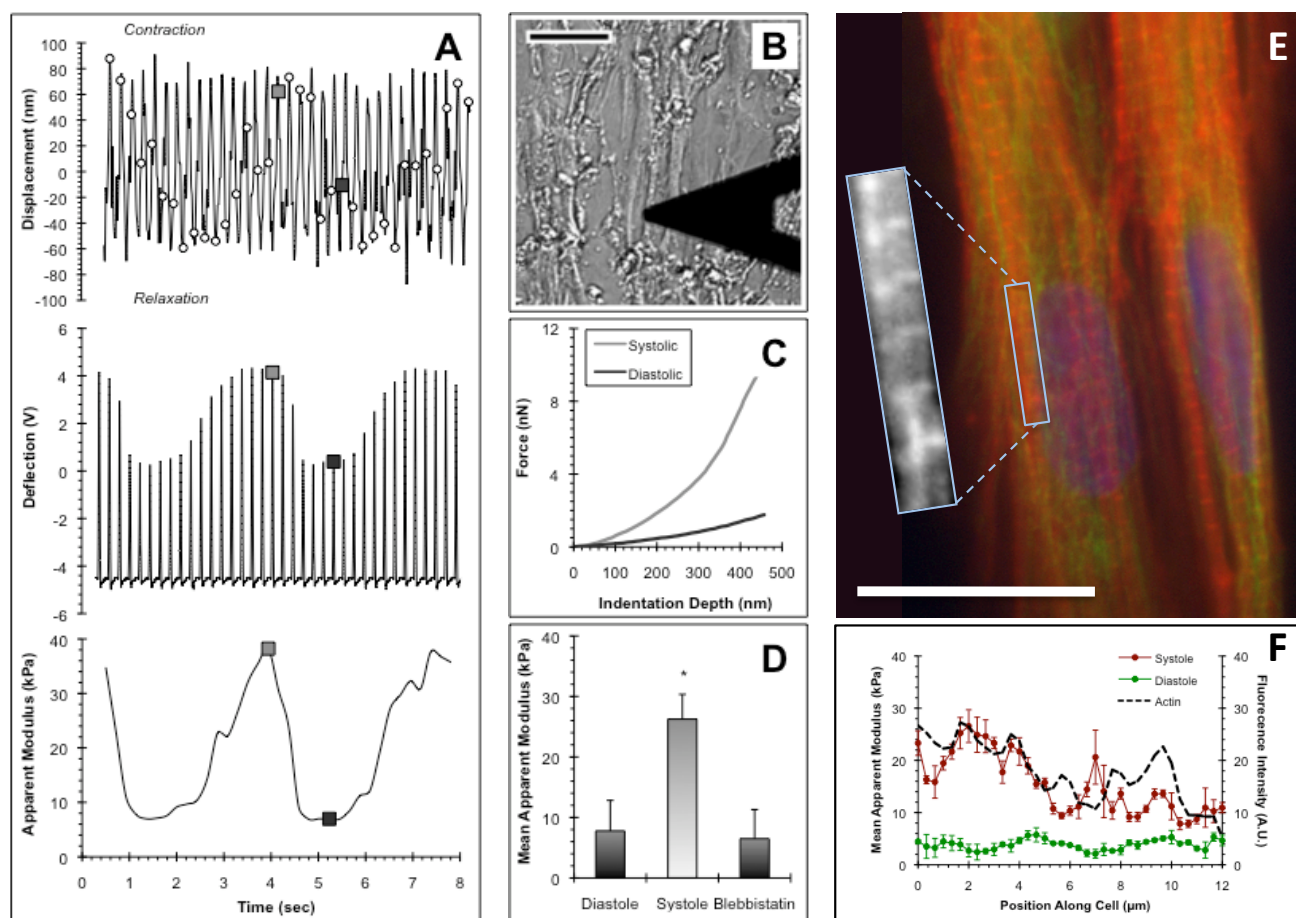


Figure 1: (A) Time course of axial displacement of a spontaneously contracting cardiomyocyte ($f_{\text{cell}} = 4.1$ Hz), where each AFM indentation time-point is indicated with a circle (top); raw continuous deflection signal from the AFM ($f_{\text{AFM}} = 4.35$ Hz) reflects changes of both cell stiffness and height (middle); corresponding time course of pointwise apparent elastic modulus at an indentation depth of 400 nm (bottom, $f_{\text{envelope}} = f_{\text{AFM}} - f_{\text{cell}} = 0.25$ Hz). (B) Bright field image of AFM indenting a cardiomyocyte. Scale bar = 20 μm . (C) Representative systolic and diastolic force-depth curves obtained from a single location on the cell. Corresponding indentation times are shown in panel A with color-coded square markers. (D) Mean apparent modulus during systole was greater than during diastole (* $p < 0.01$), which was not different from blebbistatin treatment ($p = 0.89$). (E) Pseudocolor immunofluorescence image of cardiac myocytes stained for f-actin (red), beta tubulin (green) and nucleus (blue). Scale bar = 20 μm . Spatiotemporal mechanics were mapped along 12 μm of the major axis of one cell (box with magnified actin inset). (F) A cyclic pattern emerged in pointwise modulus during systole, but not in diastole, which had a significant correlation with the banded pattern of actin in the underlying myofibrils ($p < 0.01$).

location on the cell. There are limitations to this technique. In practice, the total time for obtaining adequately sized arrays was approximately 2 minutes, which necessitates steady state contractions for that given time. Another limitation is that because data were pooled from multiple cells, regardless of their spontaneous pulse rate, any effects due to cell viscoelasticity or frequency-dependent contractile processes were hidden within the averaged stiffness values. The technique can accommodate electrical pacing for rate-controlled experiments. However, the measured properties would not be of spontaneously beating cells, which prior AFM studies suggest may differ from uniformly contracting paced cells [13].

TABLE I
YOUNG'S MODULI FOR RAT CARDIAC STRUCTURES MEASURED BY AFM

Sample	Young's Modulus	Source
Isolated beating neonatal rat cardiac myocytes	11.6±6.1 kPa (diast.)	Current study (assuming $\nu = 0.5$)
	39.4±7.6 kPa (syst.)	
Isolated neonatal rat cardiac myofibrils	61 kPa (relaxed)	Akiyama <i>et al.</i> , 2006 [1]
	145 kPa (rigor)	
Isolated passive adult rat cardiac myocytes	35.1±0.7 kPa (4 mo)	Lieber <i>et al.</i> , 2004 [3]
	42.5±1 kPa (30 mo)	
Sectioned adult rat myocardium	18±2 kPa (normal)	Berry <i>et al.</i> , 2006 [4]
	55±15 kPa (infarct)	

IV. CONCLUSION

We present an AFM technique and its application for spatiotemporal transverse stiffness mapping in isolated spontaneously contracting neonatal rat cardiomyocytes. The apparent elastic modulus varied continuously through the twitch cycle, yielding equivalent Young's moduli that ranged from about 12 kPa in diastole to 40 kPa in systole. Subcellular elastic properties exhibited higher spatial heterogeneity during systole than diastole. Blebbistatin treatment prevented contractions completely and reduced mean cellular stiffness to diastolic values, consistent with activation of acto-myosin crossbridges causing the increase in cellular transverse stiffness during systole. Moreover, the periodic sarcomeric structure of the underlying molecular contractile apparatus was detected as variations in stiffness along the length of the living cell. This may provide mechanical cues to neighboring cells in intact myocardium, possibly facilitating registration of sarcomeres in adjacent cardio-myocytes or impacting transverse active force generation and other aspects of myocardial structure and function.

ACKNOWLEDGMENTS

The authors thank Dr. Jeffrey W. Holmes for helpful discussions, Dr. Eun Jung (Alice) Lee and Do Eun Kim for assistance with myocyte isolation, and Dr. Barclay Morrison, III and Benjamin S. Elkin for technical assistance with high-speed video equipment.

REFERENCES

- [1] N. Akiyama, Y. Ohnuki, Y. Kunioka, Y. Saeki, and T. Yamada, "Transverse stiffness of myofibrils of skeletal and cardiac muscles studied by atomic force microscopy," *J Physiol Sci*, vol. 56, (no. 2), pp. 145-51, Apr 2006.
- [2] K.D. Costa, Y. Takayama, A.D. McCulloch, and J.W. Covell, "Laminar fiber architecture and three-dimensional systolic mechanics in canine ventricular myocardium," *Am J Physiol*, vol. 276, (no. 2 Pt 2), pp. H595-607, Feb 1999.
- [3] S.C. Lieber, N. Aubry, J. Pain, G. Diaz, S.-J. Kim, and S.F. Vatner, "Aging increases stiffness of cardiac myocytes measured by atomic force microscopy nanoindentation," *Am J Physiol Heart Circ Physiol*, vol. 287, (no. 2), pp. H645-651, August 1, 2004 2004.
- [4] M.F. Berry, A.J. Engler, Y.J. Woo, T.J. Pirolli, L.T. Bish, V. Jayasankar, K.J. Morine, T.J. Gardner, D.E. Discher, and H.L. Sweeney, "Mesenchymal stem cell injection after myocardial infarction improves myocardial compliance," *Am J Physiol Heart Circ Physiol*, vol. 290, (no. 6), pp. H2196-203, Jun 2006.
- [5] D.H. Lin and F.C. Yin, "A multi-axial constitutive law for mammalian left ventricular myocardium in steady-state barium contracture or tetanus," *J Biomech Eng*, vol. 120, (no. 4), pp. 504-17, Aug 1998.
- [6] H.R. Halperin, J.E. Tsitlik, B.K. Rayburn, J.R. Resar, J.Z. Livingston, and F.C. Yin, "Estimation of myocardial mechanical properties with dynamic transverse stiffness," *Adv Exp Med Biol*, vol. 346, pp. 103-12, 1993.
- [7] S. Nishimura, S. Nagai, M. Katoh, H. Yamashita, Y. Saeki, J. Okada, T. Hisada, R. Nagai, and S. Sugiura, "Microtubules modulate the stiffness of cardiomyocytes against shear stress," *Circ Res*, vol. 98, (no. 1), pp. 81-7, Jan 6 2006.
- [8] J.G. Jacot, A.D. McCulloch, and J.H. Omens, "Substrate stiffness affects the functional maturation of neonatal rat ventricular myocytes," *Biophys J*, vol. 95, (no. 7), pp. 3479-87, Oct 2008.
- [9] A.J. Engler, C. Carag-Krieger, C.P. Johnson, M. Raab, H.Y. Tang, D.W. Speicher, J.W. Sanger, J.M. Sanger, and D.E. Discher, "Embryonic cardiomyocytes beat best on a matrix with heart-like elasticity: scar-like rigidity inhibits beating," *J Cell Sci*, vol. 121, (no. Pt 22), pp. 3794-802, Nov 15 2008.
- [10] P.J. Hunter, E.J. Crampin, and P.M. Nielsen, "Bioinformatics, multiscale modeling and the IUPS Physiome Project," *Brief Bioinform*, vol. 9, (no. 4), pp. 333-43, Jul 2008.
- [11] U.G. Hofmann, C. Rotsch, W.J. Parak, and M. Radmacher, "Investigating the cytoskeleton of chicken cardiocytes with the atomic force microscope," *J Struct Biol*, vol. 119, (no. 2), pp. 84-91, Jul 1997.
- [12] A.B. Mathur, A.M. Collinsworth, W.M. Reichert, W.E. Kraus, and G.A. Truskey, "Endothelial, cardiac muscle and skeletal muscle exhibit different viscous and elastic properties as determined by atomic force microscopy," *J Biomech*, vol. 34, (no. 12), pp. 1545-53, Dec 2001.
- [13] J. Domke, W.J. Parak, M. George, H.E. Gaub, and M. Radmacher, "Mapping the mechanical pulse of single cardiomyocytes with the atomic force microscope," *Eur Biophys J*, vol. 28, (no. 3), pp. 179-86, 1999.
- [14] S.G. Shroff, D.R. Saner, and R. Lal, "Dynamic micromechanical properties of cultured rat atrial myocytes measured by atomic force microscopy," *Am J Physiol Cell Physiol*, vol. 269, (no. 1), pp. C286-292, July 1, 1995 1995.
- [15] E.J. Lee, E. Kim do, E.U. Azeloglu, and K.D. Costa, "Engineered cardiac organoid chambers: toward a functional biological model ventricle," *Tissue Eng Part A*, vol. 14, (no. 2), pp. 215-25, Feb 2008.
- [16] E.U. Azeloglu, Y.H. Yun, A.E. Saltman, I.B. Krukenkamp, F.P. Chiang, W. Chen, and G.R. Gaudette, "High resolution mechanical function in the intact porcine heart: mechanical effects of pacemaker location," *J Biomech*, vol. 39, (no. 4), pp. 717-25, 2006.
- [17] K.D. Costa, "Imaging and probing cell mechanical properties with the atomic force microscope," *Methods Mol Biol*, vol. 319, pp. 331-61, 2006.
- [18] M. Kovacs, J. Toth, C. Hetenyi, A. Malnasi-Csizmadia, and J.R. Sellers, "Mechanism of blebbistatin inhibition of myosin II," *J Biol Chem*, vol. 279, (no. 34), pp. 35557-63, Aug 20 2004.
- [19] I. Sack, J. Rump, T. Elgeti, A. Samani, and J. Braun, "MR elastography of the human heart: Noninvasive assessment of myocardial elasticity changes by shear wave amplitude variations," *Magn Reson Med*, Dec 18 2008.